Evidence for an active oxygen species on Au/TiO2(110) model catalysts during investigation with in situ X-ray photoelectron spectroscopy

K. Dumbuya, Gregory Cabailh, R. Lazzari, J. Jupille, L. Ringel, M. Pistor, O. Lytken, H.-P. Steinrück, J.M. Gottfried

Evidence for an Active Oxygen Species on Au/TiO_2(110) Model Catalysts during Investigation with *in-situ* X-ray Photoelectron Spectroscopy

K. Dumbuya[1], G. Cabailh[2], R. Lazzari[2], J. Jupille[2], L. Ringel[1], M. Pistor, O. Lytken, H.-P. Steinrück[1], J. M. Gottfried[1*]

[1]Lehrstuhl für Physikalische Chemie II, Universität Erlangen-Nürnberg, Egerlandstrasse 3, 91058 Erlangen, Germany

[2]Institut de Nanosciences de Paris, Université Paris 6 – UPMC and CNRS, 4 Place Jussieu, 75005 Paris, France

Dedicated to Prof. Dr. Frigyes Solymosi on the occasion of his 80th birthday.

CORRESPONDING AUTHOR
PD Dr. Michael Gottfried
Lehrstuhl für Physikalische Chemie II
Universität Erlangen-Nürnberg
Egerlandstraße 3, D-91058 Erlangen, Germany
Tel: +49-9131-8527320
Fax: +49-9131-8528867
Email: michael.gottfried@chemie.uni-erlangen.de

Abstract

The influence of oxygen (O_2) and carbon monoxide (CO) on Au nanoparticles supported on TiO_2(110) in the size range of 2 to 3 nm has been studied using X-ray photoelectron spectroscopy (XPS) and *in-situ* (high pressure) XPS at 300 K for O_2 and/or CO pressures of 0.1 to 1 mbar. These experiments were aimed at revisiting Au 4f core level shifts as reported in the literature and most importantly, to establish the dependence of the core-level shifts on the knowledge that there exists a maximum in reactivity for CO oxidation. Two samples were prepared with a coverage corresponding to that maximum (Au coverage 0.14-0.2 ML, particle size ~ 2 nm) while a third sample was expected to be less reactive (Au coverage 0.4 ML, particle size ~ 3 nm). At elevated O_2 pressures, a new component at higher binding energy (+2.4 eV relative to the Au(0) bulk signal) evolved at all particle sizes. Its appearance was attributed to a photoinduced activation of oxygen and a further oxidation of gold. The activation was much more efficient on the 2 nm particles. The relative intensity of the shifted component depended strongly on O_2 pressure and, thus, likely on the coverage; not present in 0.1 mbar O_2 regardless of exposure time and particle size, it dominated the Au 4f spectrum of particles 2 nm in size. This pressure-dependent formation reconciles previously conflicting XPS data. Finally, the oxygen activated species were very reactive toward CO as manifested by the rapid disappearance of the new Au 4f component in a 1:1 mixture of CO and O_2. The rates of evolution and consumption of this component were found to depend on gold coverage (and thus, particle size) and were highest for the smaller particles.

1. Introduction

Since its discovery, the origin of the catalytic activity of oxide-supported gold particles has been a matter of vivid controversy. Many efforts have been devoted to understanding the mechanistic aspects behind the unusually high catalytic activity of gold, in particular regarding the prototypical oxidation of CO. The interest in the CO oxidation reaction stems from potential practical applications in, for example, the purification of H_2 streams by selective oxidation of CO in order to avoid deactivation of Pt fuel cells. Since early reports by Haruta *et al.* [1], who showed the direct dependence of the catalytic activity on the Au cluster size, a series of models have been put forward, all in an effort to disentangle the mechanistic pathway of CO oxidation on Au. Today, there is a general consensus that the catalytic activity decreases drastically for particle sizes above 5 nm [2,3]. It is also nowadays a widely accepted view that the support material plays a significant role in the process by influencing the morphology and electronic configuration of the Au particles [4-7] although some groups advocate a lesser role of the support [8].

Numerous experimental methods have been applied in the search for the active site in the CO oxidation over supported gold catalysts. Photoelectron spectroscopy has been widely used in this regard, mainly because changes in the electronic state of small metal clusters can be routinely monitored using this technique. Lately, *in-situ* implementations of this method have gained momentum due to their potential to identify mechanistically important transient species during reaction conditions. By *in-situ* photoemission spectroscopy (*in-situ* XPS) using an Au/TiO_2 powder catalyst, Willneff *et al*. [9] observed Au 4f core level shifts of +0.3 eV and +0.9 eV, which they assigned to bulk-like metallic gold and to intermediate gold species, respectively. The former is close to the 0.3-0.4 eV shift reported by Herranz *et al*. [10] when $Au/TiO_2(110)$ was exposed to a CO/O_2 mixture. Under the same *in-situ* conditions but with Au nanoparticles on a silica support, the same authors have also described a +0.3 eV shift of the Au 4f level at 150 °C, but no such shift was found at room temperature.

Jiang *et al*. reported a very different Au 4f core-level shift of 2.3 eV toward higher binding energies when Au particles or Au foil were exposed to 1 Torr O_2 during in-situ X-ray photoelectron spectroscopic measurements [11]. These results were explained by photon and photoelectron induced dissociative chemisorption of oxygen, in agreement with previous observations [12]. Similar Au 4f shifts have been observed for Au particles on TiO_2 and SiO_2 oxidized by oxygen plasma. Related temperature-programmed desorption (TPD) measurements confirmed that these shifts are due to chemisorbed atomic oxygen and gold oxide [13-15]. Beyond the fact that the observations of Jiang *et al.* deviate from those of

Willneff *et al.*, the conflicting results also question the applicability of in-situ XPS to analyze the catalytic reaction itself [9,11].

By a simultaneous study of the reactivity and the particle morphology (size and shape), it has recently been shown [16] that the rate of the catalytic oxidation of CO on $Au/TiO_2(110)$ films passes through a maximum for particles of 2-2.5 nm in diameter. On the basis of these findings, we have investigated $Au/TiO_2(110)$ samples with different Au particle sizes representative of highly as well as poorly active conditions by *in-situ* XPS in the presence of O_2, CO and a mixture of both gases in the 0.1–1 mbar range. These experiments were aimed at revisiting Au 4f core level shifts as reported in the literature and to establish the dependence of the core-level shifts on the previously determined reaction rates. To address this issue systematically, three different $Au/TiO_2(110)$ model catalysts were prepared, with particles close to the optimum size (1.6 to 2.2 nm in size), and larger than the optimum size (~3 nm). The Au 4f, O 1s and Ti 2p levels were systematically recorded. In our experiments, previously reported Au core level shifts were convincingly reproduced. In addition, we observe the two separate Au 4f core level shifts during a single experiment, unlike previous reports [9-11], and show that the 0.9 eV shift, whose origin has been controversially discussed in the literature (Au (I) oxide [17,18] versus final state effects [19-23]) is most likely due to final state effects.

2. Experimental

The XPS chamber used for photoelectron and *in-situ* photoelectron investigations of the Au/TiO_2 system is a complex equipment that allows conventional UHV experiments but also high pressure XPS (with reactive gas background pressures of up to 1 mbar) [24]. The key feature of this equipment is the efficient combination of four differential pumping stages between the sample (electron emission) and analyzer (electron detection) stages. The analyzer is a modified Omicron EA-125 unit and the X-ray source is a modified dual anode source (Specs XR-50) whose vacuum environment is completely isolated from that of the analysis chamber with the help of a 3 μm thick Al foil and additional gasket seals. The photon flux was approximately 4×10^9 photons/(cm^2·s). Gas dosing is achieved via flooding the main chamber (background dosing) with the required gas or via two capillary tubes that are directed at the surface of the sample (beam dosing). The background dosing method was utilized in this work. The base pressure in this chamber is in the low 10^{-9} mbar regime. A detailed description of this system is available in the work of Pantförder *et al*. [24]

The crystal was mounted on a transferable home-made sample holder system, with the aid of which temperatures up to 1200 K are attainable via resistive heating. The temperature was measured using a thermocouple pair (type K) glued to the side of the crystal with ceramic glue (Aremco Ultra-Temp 516). The sputter source is a filament-free plasma device (Tectra) that enables sample bombardment in both inert gas and reactive gas environments. All sample preparation and Au evaporation were performed in a separate preparation chamber with a base pressure of 3×10^{-10} mbar. This chamber was also fitted with LEED optics (Varian), which was used to confirm the presence of a well-ordered TiO_2(110) surface, and a quadrupole mass spectrometer (Pfeiffer Prisma) for monitoring background gas concentrations.

Prior to each deposition episode, the TiO_2(110) single crystal was prepared by cycles of bombardment with Ar^+ ions and annealing to 820°C for 15 minutes in an oxygen environment (5×10^{-6} mbar) according to established preparation procedures [25-28]. Au nanoparticles used in this study were prepared *in-situ* via vapor deposition of gold under ultrahigh-vacuum (UHV) conditions on a rectangular ($12\times10\times1$ mm^3) TiO_2(110) single crystal surface. The evaporator was a home-built Knudsen cell based on a ceramic tube which was filled with Au wire (99.999%, Goodfellow). Tungsten wire (0.2 mm thick) was wound along the tube for resistive heating. The temperature of the cell was measure by a type K thermocouple. Gold coverages were checked by three independent approaches, namely quartz microbalance, analysis of the damping of the XPS signal, and absolute calibration of the Au 4f signal with respect to the Au 4f peak collected on a Au(111) crystal. Two model catalysts with gold coverages of 0.14 ML and 0.2 ML were prepared to reproduce the coverage at which the maximum in catalytic activity for CO oxidation was observed (0.2 ML with particles of 2.1 nm in size) [16]. A third sample with a coverage of 0.4 ML is expected to correspond to about half the reactivity of the 2 nm particles. As for the relationship between size and coverage, Laoufi *et al.* found particles of 2.1 and 4.2 nm in size for coverages of 0.2 and 1.0 ML, respectively, in agreement with Lai *et al.* [29] who found 2 nm, 3 nm and 3.7 nm for coverages of 0.1 ML, 0.25-5 ML and 1.0 ML. This is also in agreement with reports by Valden *et al.* [30]. Based on these previous reports, the coverages of 0.14-0.2 ML and 0.4 ML used herein are assumed to correspond to particles of ~ 2 nm and 3 nm in size, respectively.

Photoemission spectra of the Au 4f, Ti 2p, O 1s, and C 1s regions were recorded using Al Kα radiation (1486.6 eV). The binding energies (BE) of all Au 4f core levels were corrected using the Ti $2p_{3/2}$ binding energy of 459.0 eV to account for residual charging effects. This BE value was previously established for a TiO_2(110) single crystal with sufficient conductivity to prevent charging under similar experimental conditions (analyzer transmission function,

sample position, anode type and power). The Au spectra were fitted using a combination of Gaussian and Lorentzian curves (pseudo Voigt function). Prior to peak deconvolution, a Shirley background was subtracted from all spectra. A $4f_{7/2}$ and $4f_{5/2}$ spin orbit splitting value of 3.65 eV and an area ratio 4:3 were fixed for all fits.

3. Results and discussion

3.1. 0.4 ML Au on TiO_2(110): Nanoparticles larger than the optimum size (~ 3.0 nm)

Figure 1 shows Au 4f spectra for a sample with a Au coverage of 0.4 ML, which corresponds to Au nanoparticles with an average diameter of ~3 nm, *i.e.* particles larger than the optimum size [16]. In Figure 1a, the Au $4f_{7/2}$ peak maximum is centered at 83.9 eV. There is an additional minority species with a maximum at 85.2 eV (brown curves), which has been observed previously [10]. The major Au $4f_{7/2}$ component can be assigned to metallic Au, while the nature of the minor component is controversial, as various authors have attributed this signal either to Au(I) [10,17,18] or to the finite size of the clusters combined with the insulating nature of the substrate, which results in a less efficient screening of the final core hole [18-23] such that the positive Au 4f core-level shift induced by the final state charge outweighs the negative surface atom core-level shift [31]. When this sample was exposed to molecular oxygen (0.1 mbar, Figure 1b) under X-rays for one hour, the main peak shifted by 0.3 eV towards higher binding energy. The same shift was observed for Au/TiO_2 in a CO/O_2 mixture (partial pressures 0.1 Torr) at 150°C and attributed to the adsorption of CO, which was proposed to withdraw electron density from the Au particles [10]. The fact that we find the same shift in a pure O_2 atmosphere suggests that it is related to an oxygen equilibrium coverage rather than carbon monoxide adsorption. At 0.1 mbar and regardless of exposure time, no other Au 4f component was observed, in agreement with the findings by Willneff *et al*. [9].

During the first 10 minutes of oxygen exposure at 1 mbar (Figure 1c), the main peak shifted further to higher binding energy by 0.2 eV relative to the peak at an O_2 pressure of 0.1 mbar and 0.5 eV relative to its UHV counterpart. The general intensity loss in 1 mbar O_2 is due to damping of the photoelectrons by the gas phase (compare Figure 1a and 1c). About 40 minutes later under the same conditions, a strong new doublet whose signature dominated the entire spectrum evolved at 86.5 eV and 90.2 eV, respectively (Figure 1d, blue curves). We trace the origin of this species to the formation of chemisorbed atomic oxygen and (at higher coverages) of gold oxide as a result of the activation of molecular oxygen by photoelectrons and X-ray photons, as was hitherto suggested by Jiang *et al*. [11]. This observation is in line

with previous studies on the activation of physisorbed O_2 on Au(110) by irradiation with UV photon or electrons, resulting in the formation of chemisorbed oxygen and gold oxide [32,33]. The subsequent XPS measurement under UHV conditions (~ 5×10^{-8} mbar) revealed that the main Au 4f peak is still shifted towards higher binding energy by 0.3 eV with respect to the initial UHV measurement. A similar observation was made previously, following exposure of a reduced TiO_2(110) sample to 20 mbar O_2 and subsequent XPS analysis in UHV (not shown). Moreover, the component at 86.5 eV shifted negatively by 0.7 eV toward lower binding energy following O_2 removal. This shift is most likely related to the formation of a non-stoichiometric, oxygen deficient Au-oxide species due to either reaction with background reductants such as CO or (see Figure 2) to an X-ray induced reductive decomposition of the oxide. The overall weight of this component decreases with respect to the overall Au 4f signal.

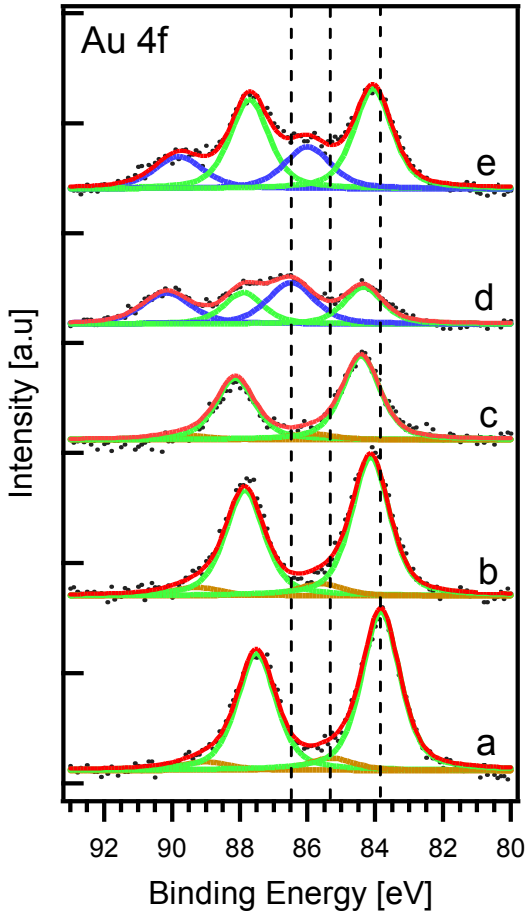

Figure 1. XP and *in-situ* XP spectra of the Au 4f region of 0.4 ML Au (~3 nm Au clusters) on TiO_2 (110). (a) As-prepared Au particles on TiO_2(110) at 300 K in UHV; (b) *in-situ* XPS in 0.1 mbar O_2, 1 hour total exposure to X-rays; (c) *in-situ* XPS in 1 mbar O_2, 10 minutes exposure to X-rays; (d) *in-situ* XPS in 1 mbar O_2, 1 hour exposure to X-rays; (e) UHV XPS measurement following the *in-situ* experiment (d).

3.2. 0.2 and 0.14 ML Au on TiO_2(110): Nanoparticles close to the optimum size (~ 2 nm)

XPS and in-situ XPS data for particles in the size range with maximum CO oxidation activity are presented in Figure 2. The changes in the Au 4f spectra of 0.2 ML Au on TiO_2 (110) (particles of ~ 2 nm in size) during exposure to reactive gases and simultaneous XPS measurements differ from the corresponding data for larger Au particles (cf. Figure 1). The Au $4f_{7/2}$ peak appeared at 84.1 eV (green curves), 0.2 eV higher than the binding energy position of the larger particles (0.4 ML Au, ~3.0 nm, Figure 1). Again, this trend is expected for small metal clusters supported on insulating substrate due to the already mentioned less efficient core hole screening with decreasing particle size. Furthermore, exposure of these particles to 0.1 mbar oxygen caused a shift toward lower binding energy of ~0.2 eV, but no visible evolution of Au oxide, similar to the findings for the larger particles. In 1 mbar oxygen, Au oxide was rapidly formed (Figure 2c) during the first ten minutes of exposure, in stark contrast to the situation for larger particles (cf. Figure 1c). After O_2 exposure at 1 mbar for 1 hour (Figure 2d), over 95 % of existing Au species were already in the oxidized state (Au $4f_{7/2}$ binding energy of 86.6 eV), much more than in the case of the higher Au coverage (55% in the oxidized state, cf. Figure 1d). These observations, in particular Figure 2c, indicate that activation of molecular oxygen is much more efficient than on the larger particles. Based on the widely accepted Langmuir-Hinshelwood mechanism for CO oxidation on Au, activation of dioxygen is considered to be a key step, followed by the consumption of atomic oxygen species by adsorbed CO to produce CO_2. On the real catalyst, this activation takes place spontaneously, whereas in our experiments, oxygen activation leading to chemisorbed oxygen and gold oxide is mainly photoinduced. (Note that no formation of chemisorbed oxygen was observed in control experiments during which the sample was exposed to the same dosages of oxygen *without* simultaneous exposure to X-rays.) The rate of the photoinduced formation of chemisorbed oxygen and gold oxide appears to be related to the particle size in a similar way as is the rate for the spontaneous CO oxidation. Possibly, both effects have a common origin. If, for example, the 2 nm particles form the strongest bonds to O_2 molecules, this would explain the most efficient O_2 activation for the spontaneous CO oxidation, but also (due to the thus increased O_2 equilibrium coverage) the more efficient photoinduced formation of chemisorbed oxygen or gold oxide.

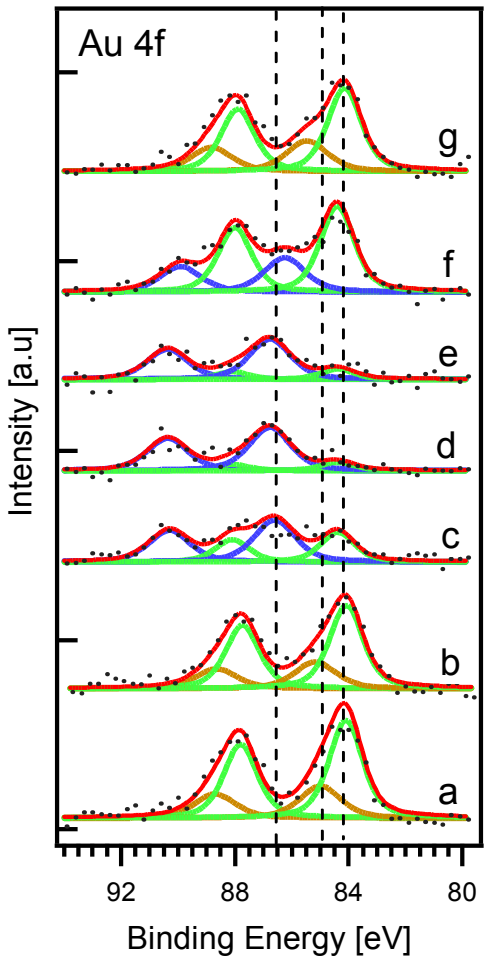

Figure 2: XP and *in-situ* XP spectra of Au 4f region of 0.2 ML Au (~ 2.0 nm Au clusters) on TiO_2 (110). (a) As-prepared Au particles on TiO_2(110) at 300 K in UHV; (b) *in-situ* XPS in 0.1 mbar O_2, 1 hour total exposure to X-rays; (c) *in-situ* XPS in 1 mbar O_2, 10 minutes exposure to X-rays; (d) in-situ XPS in 1 mbar O_2, 1 hour exposure to X-rays; (e) after (d), but without X-rays for 30 minutes at 1 mbar O_2,; (f) UHV XPS measurement after exposure to X-rays for 30 minutes in UHV; (g) UHV XPS measurement after 1 hour in UHV.

It is noteworthy that the synchrotron experiments by Herranz *et al.* [10] and Jiang *et al*. [11] were run with a much higher photon flux (~4×10^{14} photons/(cm^2·s)) than our experiment, ~4×10^{9} photons/(cm^2·s). The X-ray exposure of 10 minutes reported in ref. 11 corresponded to a total photon dose of 2.4×10^{17} photons/cm^2, whereas an exposure of 1 hour in our experiment corresponds to a photon dose of only 1.5×10^{13} photons/cm^2. However, the 2.4 eV Au 4f peak, which is assumed to be caused by X-ray induced oxygen activation is not seen under a pressure of 0.1 mbar O_2 whatever the photon flux (compare Figures 1b and 2b to data collected by Herranz *et al*. [10]). As seen in Figures 1d and 2c to 2g, the 2.4 eV shift appears herein under a pressure of 1 mbar, in line with the observations of Jiang *et al*. [11]. Therefore, the formation of the activated oxygen species does not depend on the X-ray beam flux but

rather on the oxygen pressure and, consequently, on the oxygen pressure alone. Apparently, the rate-limiting factor is the O_2 equilibrium coverage rather than the photon intensity. Considering the very low adsorption energy of O_2 on Au surfaces (below 12 kJ/mol) [12] it is clear that the O_2 equilibrium coverage must be very low even at 1 mbar O_2.

Finally, it was found that the intensity of the chemisorbed oxygen (or gold oxide) peak did not change when the X-ray source was shut down for 30 minutes. This suggests that oxygen chemisorption continues under these conditions, because otherwise the intensity of this peak would have decreased due to reaction with background CO (Figure 2e). This is in agreement with previous reports by Deng *et al.* [34] who found that the dissociation probability of O_2 on Au(111) is dramatically increased by the presence of atomic oxygen on the surface.

Exposure to X-ray photons in UHV removed atomic oxygen (Figure 2f). However, in the absence of photons and O_2, the Au oxide is suggested to be rapidly reduced by background CO (cf. Figures 1e and 2g), in agreement with the previously observed high reactivity of chemisorbed atomic oxygen and gold oxide toward CO [32,33] and with the results presented in the following section.

3.3 Au nanoparticles close to the optimum size under reactive conditions

Having gained insight into the behaviour of the catalytically more active Au particles in oxygen in the 0.1-1 mbar regime, it was necessary to investigate these under CO oxidation conditions with *in-situ* XPS. The results are presented in Figure 3. In the as-prepared sample, typical Au $4f_{7/2}$ binding energies of 84.1 eV and 85.0 eV are clearly evident. Comparison of Figures 1a, 2a and 3a reveals that the relative intensities of the 85.0 eV components increase with decreasing Au coverage (and thus, decreasing cluster size).

In Figure 3a and 3b, the green and brown curves depict metallic gold species, in line with observations from the first two experiments. The key message again is that 0.1 mbar O_2 exposure does not cause gold oxide formation irrespective of particle size and duration of photon and oxygen exposure. However, like in the case of the 2 nm clusters, a small shift toward lower binding energy was recorded in 0.1 mbar O_2. This observation suggests that below a threshold size (which is apparently between 2 and 3 nm), the formation of negatively charged gold particles on titania in oxygen is enhanced, presumably due to transfer of electron density from the underlying oxide substrate [35]. The evolution of Au_2O_3 was also observed in 0.5 mbar oxygen: after 1 hour exposure, ~50% of the metallic gold were converted to the oxide (Figure 3c). When 0.5 mbar CO were introduced to the system already containing 0.5 mbar oxygen, the oxidic gold component was rapidly consumed while the signal of metallic

gold evolved simultaneously (Figure 3d). From recent experiments using the same gold coverage, more than 50 % of the oxidic component is consumed in the first two minutes of CO exposure. When CO was shut off again, while the exposure to O_2 (0.5 mbar) continued, the signal component of oxidic gold re-emerged (Figure 3e). Note that the oxide that reappeared on the surface in 0.5 mbar O_2 (Figure 3e) was completely consumed by background gases after one hour, while the component around 85 eV (brown curve) resurfaced to full intensity. The continued presence of this species under reducing UHV conditions, where the Au(III) oxide easily reacts with CO, supports the conclusion that it is not Au in an oxidized state. Instead, its origin may be traced back to poorly screened gold atoms, either due to the presence of very small clusters in the size distribution or due to gold atoms at the periphery of the (larger) clusters.

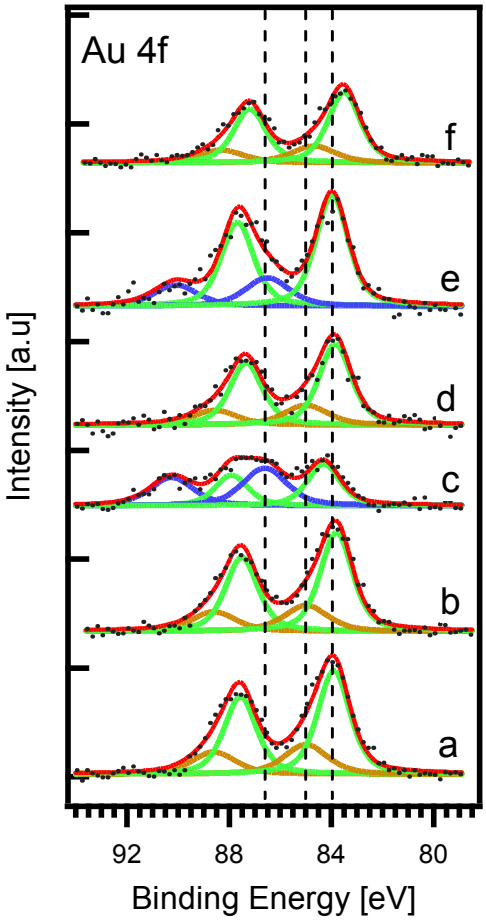

Figure 3: XP and *in-situ* XP spectra of Au 4f region of 0.14 ML Au (~ 1.6-1.8 nm Au clusters) on TiO_2 (110). (a) As-prepared Au particles on TiO_2(110) at 300 K in UHV; (b) *in-situ* XPS in 0.1 mbar O_2, 1 hour total exposure to X-rays; (c) in-situ XPS in 0.5 mbar O_2, 1 hour exposure to X-rays; (d) *in-situ* XPS in a 1:1 mixture of CO + O_2, 1 mbar, 1 hour total exposure to X-rays; (e) *in-situ* XPS in 0.5 mbar O_2 (CO off); (f) UHV XPS measurement after 1 hour in UHV (O_2 and CO off).

Conclusions

Three Au/TiO_2(110) models catalysts were exposed to various partial pressures of oxygen (up to 1 mbar) and to reactive CO + O_2 mixture and simultaneously analyzed by *in-situ* photoelectron spectroscopy. Based on the knowledge that there is a reactivity maximum for CO oxidation, two samples were prepared with a coverage corresponding to that maximum (coverage 0.14-0.2 ML, particle size ~ 2 nm) while a third sample was expected to be less reactive (coverage 0.4 ML, particle size ~ 3 nm). The main observations made in this study can be summarized as follows:

(a) Upon exposure of large particles (~ 3 nm) to 0.1 mbar of oxygen, the Au 4f core level shifts by 0.2-0.5 eV toward higher binding energy, which is attributed to charge transfer arising from oxygen adsorption either on the gold particles or at the interface between particles and substrate. Such shift, which is an order of magnitude lower than that expected for gold oxide, suggests molecular adsorption of oxygen in the presence of 0.1 mbar O_2 in the gas phase.

(b) Upon a similar oxygen pressure, Au 4f levels of particles of ~2 nm in size shift toward lower binding energy (-0.2 to -0.4 eV). The origin of this shift seems to be closely related to particle size; it is absent when larger particles are used, but appears in both samples with particles in the 2 nm size range. This shift can be understood on the basis of a negative charge transfer to Au particles from the substrate (cluster size effect). Apparently, the effect of this transfer is much more pronounced on the smaller particles.

(c) Exposures to oxygen at pressures of 0.5 to 1.0 mbar lead to the appearance of a new component in the Au 4f signal, which is shifted by 2.4 eV relative to the Au(0) signal. This additional contribution is assigned to the formation of chemisorbed oxygen and gold oxide (Au_2O_3) due to photon and photoelectron induced dissociation of dioxygen. By comparison with data from other groups, the formation of this species is shown to strongly depend on the oxygen pressure (the 2 nm particles are fully transformed after 1 hour under 1 mbar of oxygen while the species is not observed under 0.1 mbar) which indicates that it likely depends on the O_2 equilibrium coverage. In addition, the activation of oxygen depends on the size of the Au particles; it is much more efficient on the particle corresponding to the maximum in reactivity. Finally, the activated oxygen species was found to be very reactive toward CO. Therefore, the fraction of oxidized gold is likely determined by a balance between beam-induced formation and

removal due to reaction with background CO (or radiation/electron stimulated desorption), leading to a stationary state.

References

[1] A. Ueda, T. Ohshima, M. Haruta, Appl. Catal. B: Environ. 12 (1997) 81.

[2] G. C. Bond, D. T. Thompson, Gold Bull. 37 (2000) 74.

[3] R. Meyer, C. Lemire, S.K. Shaikhutdinov, H. Freund, Gold Bulletin 37 (2004) 72.

[4] A. Kolmakov, D. W. Goodman, Surf. Sci. Lett. 490 (2001) L 597.

[5] B. Yoon, H. Häkkinen, U. Landman, A. S. Wörz, J. M. Antonietti, S. Abbet, K. Judai, U. Heinz, Science 307 (2005) 403.

[6] S. Arrii, F. Morfin, A. J. Renouprez, J. I. Rouset, J. Am. Chem. Soc. 126 (2004) 1199.

[7] R. J. H. Greisel, B. E. Nieuwenhuys, J. Catal. 199 (2001) 48.

[8] N. Lopez, T. V. W. Jansens, B. S. Clausen, Y. Xu, M. Mavrikakis, T. Bligaard, J. K. Norskov, J. Catal. 223 (2004) 232.

[9] E. A. Willneff, S. Braun, D. Rosenthal, H. Bluhm, M. Hävecker, E. Kleimenov, A. Knop-Gericke, R. Schlögl, S. L. M. Schroeder, J. Am. Chem. Soc. 128 (2006) 12052.

[10] T. Herranz, X. Deng, A. Cabot, P. Alivisatos, Z. Liu, G. Soler-Illia, M. Salmeron, Catalysis Today 143 (2009) 158.

[11] P. Jiang, S. Porsgaard, F. Borondics, M. Köber, A. Caballero, H. Bluhm, F. Besenbacher, M. Salmeron, J. Am. Chem. Soc. 132 (2010) 2858.

[12] J. M. Gottfried, K. J. Schmidt, S. L. M. Schroeder, K. Christmann, Surf. Sci. 511 (2002) 65.

[13] L.K. Ono, B. Roldan Cuenya, J. Phys. Chem. C 112 (2008) 4676.

[14] J.M. Gottfried, J. Phys. Chem. C 112 (2008) 16721.

[15] L.K. Ono, B.R. Cuenya, J. Phys. Chem. C 112 (2008) 16723.

[16] I. Laoufi, M-C Saint-Lager, R. Lazzari, J. Jupille, O. Robach, S. Garaudée, G. Cabailh, P. Dolle, H. Cruguel, A. Bailly, J. Phys. Chem. C, submitted.

[17] J. Knecht, R. Fischer, H. Overhof, F. Hensel, J. Chem. Soc. Chem. Comm. 21 (1978) 905.

[18] Q. Fu, H. Saltsburg, M. Flytzani-Stephanopoulos, Science 301 (2003) 935.

[19] S. Lee, C. Y. Fan, T. P. Wu, S. L. Anderson, Surf. Sci. 578 (2005) 5.

[20] L. Oberli, R. Monot, H. J. Mathieu, D. Landolt, J. Buttet, Surf. Sci. 106 (1981) 301.

[21] T. T. P. Cheung, Surf. Sci. 140, (1984) 151.

[22] H. S. Shin, H. C. Choi, Y. Jung, S. B. Kim, H. J. Song, J. Shin, Chem. Phys. Lett. 383 (2004) 418.

[23] C. N. R. Rao, A. K. Santra, V. Vijayakrischnan, Top. Catal., 1, (1994) 25.

[24] J. Pantförder, J. F. Zhu, D. Borgmann, R. Denecke, H.-P. Steinrück, Rev. Sci. Instrum. 76 (2005) 014102.

[25] R. T. Zehr, M. A. Henderson, Surf. Sci. 602 (2008) 1507.

[26] M. B. Hugenschmidt, L. Gamble, C. T. Campbell, Surf. Sci. 302 (1994) 329.

[27] R. L. Kurz, R. Stockbauer, T. E. Madey, E. Roman, J. L. de Segovia, Surf. Sci. 218 (1989) 178.

[28] J. M. Pan, B. L. Manschoff, U. Diebold, T. E. Madey, J. Vac. Sci. Technol. A 10 (1992) 2470.

[29] X. Lai, T. P. St. Clair, M. Valden, D. W. Goodmann, Progr. Surf. Sci. 59 (1998) 25.

[30] M. Valden, S. Pak, X. Lai, D. W. Goodmann, Catal. Letters 56 (1998) 7.

[31] G. K. Wertheim, S. B. DiCenzo, and S. E. Youngquist, Phys. Rev. Lett. 51 (1983) 2310.

[32] J.M. Gottfried, K.J. Schmidt, S.L.M. Schroeder, K. Christmann, Surf. Sci. 525 (2003) 184.

[33] J.M. Gottfried, K.J. Schmidt, S.L.M. Schroeder, K. Christmann, Surf. Sci. 525 (2003) 197.

[34] Y. Deng, B.K. Min, A. Guloy, C.M. Friend, J. Am. Chem. Soc. 127 (2005) 9267.

[35] N. Kruse, S. Chenakin, Appl. Catal. A: General, 391 (2011), 367.